A nomogram for predicting hyperprogressive disease after immune checkpoint inhibitor treatment in lung cancer

Shuhui Cao[1#], Yao Zhang[1#], Yan Zhou[1], Wenwen Rong[2], Yue Wang[1], Xuxinyi Ling[1], Lincheng Zhang[1], Jingwen Li[1], Yusuke Tomita[3], Satoshi Watanabe[4], Takeo Nakada[5], Nobuhiko Seki[6], Toyoaki Hida[7], Said Dermime[8], Runbo Zhong[1], Hua Zhong[1]

[1]Department of Pulmonary, Shanghai Chest Hospital, Shanghai Jiao Tong University, Shanghai, China; [2]Statistical Center, Shanghai Chest Hospital, Shanghai Jiao Tong University, Shanghai, China; [3]Department of Respiratory Medicine, Graduate School of Medical Sciences, Kumamoto University, Kumamoto, Japan; [4]Department of Respiratory Medicine and Infectious Diseases, Niigata University Graduate School of Medical and Dental Sciences, Niigata, Japan; [5]Division of Thoracic Surgery, Department of Surgery, The Jikei University School of Medicine, Tokyo, Japan; [6]Division of Medical Oncology, Department of Internal Medicine, Teikyo University School of Medicine, Tokyo, Japan; [7]Lung Cancer Center, Central Japan International Medical Center, Gifu, Japan; [8]Translational Cancer Research Facility, Translational Research Institute, National Center for Cancer Care and Research, Hamad Medical Corporation, Doha, Qatar

Contributions: (I) Conception and design: H Zhong, R Zhong, S Cao; (II) Administrative support: H Zhong, R Zhong; (III) Provision of study materials or patients: S Cao, Y Zhang, Y Zhou, Y Wang, X Ling; (IV) Collection and assembly of data: S Cao, Y Zhang, L Zhang, J Li; (V) Data analysis and interpretation: S Cao, Y Zhang, W Rong; (VI) Manuscript writing: All authors; (VII) Final approval of manuscript: All authors.
[#]These authors contributed equally to this work.

Correspondence to: Hua Zhong; Runbo Zhong. Department of Pulmonary, Shanghai Chest Hospital, Shanghai Jiao Tong University, Shanghai, China. Email: eddiedong8@hotmail.com; tonic_chung@139.com.

Background: Immune checkpoint inhibitor (ICI) therapy is an emerging type of treatment for lung cancer (LC). However, hyperprogressive disease (HPD) has been observed in patients treated with ICIs that lacks a prognostic prediction model. There is an urgent need for a simple and easily implementable predictive model to predict the occurrence of HPD. This study aimed to establish a novel scoring system based on a nomogram for the occurrence of HPD.

Methods: We retrospectively identified 1473 patients with stage III–IV LC or inoperable stage I–II LC (1147 in training set, and 326 in testing set), who had undergone ICI therapy at the Shanghai Chest Hospital between January 2017 and March 2022. Available computed tomography (CT) data from the previous treatment, before ICI administration, and at least 2 months after the first the course of ICI administration is collected to confirm HPD. Data from these patients' common blood laboratory test results before ICI administration were analyzed by the univariable and multivariable logistic regression analysis, then used to develop nomogram predictive model, and made validation in testing set.

Results: A total of 1,055 patients were included in this study (844 in the training set, and 211 in the testing set). In the training set, 93 were HPD and 751 were non-HPD. Multivariate logistic regression analyses demonstrated that lactate dehydrogenase [LDH, P<0.001; odds ratio (OR) =0.987; 95% confidence interval (CI): 0.980–0.995], mean corpuscular hemoglobin concentration (MCHC, P=0.038; OR =1.021; 95% CI: 1.003–1.033), and erythrocyte sedimentation rate (ESR, P=0.012; OR =0.989; 95% CI: 0.977–0.997) were significantly different. The prediction model was established and validated based on these 3 variables. The concordance index were 0.899 (95% CI: 0.859–0.918) and 0.924 (95% CI: 0.866–0.983) in training set and testing set, and the calibration curve was acceptable.

Conclusions: This model, which was developed from a laboratory examination of LC patients undergoing ICI treatment, is the first nomogram model to be developed to predict HPD occurrence and exhibited good sensitivity and specificity.

Keywords: Lung cancer; immune checkpoint inhibitors (ICIs); hyperprogressive disease (HPD); nomogram

Introduction

Lung cancer (LC) poses one of the greatest threats to global health, and accounts for approximately 18% of cancer cases worldwide (1). LC is usually first diagnosed with regional or distant metastases, which means it is in stage IIIB-IV (2). In addition to conventional treatments, such as surgery, chemotherapy, and radiotherapy, immune checkpoint inhibitor (ICI) therapy is emerging as a new type of treatment for LC (3-6). Immunotherapy not only plays vital roles in neoadjuvant and adjuvant therapy, but also shows satisfactory safety and promising efficacy in the treatment of advanced stage LC. However, in patients receiving immunotherapy, a response pattern known as hyperprogressive disease (HPD) has been observed in various types of tumors, including LC (7,8). HPD refers to an acceleration of disease progression after ICI administration. According to previous studies, the incidence of HPD is around 10–20% (9,10). Recently published studies have identified several potential biomarkers associated with HPD, including gene mutations of tumor cells, tumor microenvironment (TME) biomarkers, and other related indicators; however, these indicators are difficult to obtain, and histological biopsy and genetic testing were usually required, which is time- and money-consuming (11). An easier approach is needed to predict HPD. Research on the laboratory features of HPD patients is still limited, and additional efforts are needed to characterize this condition more comprehensively. To improve the screening of patients with HPD and further innovate precision medicine, we compared the clinical data like age, gender, or other clinical data of the two groups, summarized the common laboratory characteristics of patients undergoing ICI and developed and validated a predictive nomogram model of HPD. We present the following article in accordance with the TRIPOD reporting checklist (available at https://tlcr.amegroups.com/article/view/10.21037/tlcr-22-171/rc).

Methods

Patients

This retrospective analysis firstly enrolled patients at the Shanghai Chest Hospital (Shanghai, China) with pathologically confirmed LC from January 2017 to June 2021 as training set. The testing set included 211 patients treated between July 2021 and March 2022 at the Shanghai Chest Hospital. Participants were included in this study were required to meet the following inclusion criteria: (I) they had a histological diagnosis of LC according to World Health Organization (WHO) histological classification and confirmed to have stage III–IV LC or inoperable stage I-II according to the UICC/AJCC TNM Classification; (II) they had undergone ICI treatment; (II) they had an Eastern Cooperative Oncology Group's performance status (ECOG PS) of 0 to 2; (IV) they had measurable parameters for of all target lesions; and (V) there was available computed tomography (CT) data from the previous treatment, before ICI administration, and at least 2 months after the first the course of ICI administration. Response Evaluation Criteria in Solid Tumors (RECIST) 1.1 and immune-related RECIST (12) criteria were used for efficacy assessment. The study was conducted in accordance with the Declaration of Helsinki (as revised in 2013). The study was approved by institutional ethics board of Shanghai Chest hospital (No. IS2118). Individual consent for this retrospective analysis was waived.

Definition of HPD

Tumor growth rate (TGR) is the rate of monthly increase in tumor volume and was calculated according to the definition of Gomez-Roca *et al.* (13). The tumor volume (V) was approximately calculated with the following formula: $V=\pi D^3/2$, where D is the sum of the longest diameter of all target lesions. Pre-baseline tumor volume of (V_{pre}), baseline volume (V_{base}), and volume after ICI treatment (V_{ther}) were calculated based on imaging material. The time of pre-baseline, baseline, and post-ICI treatment were defined as T_{pre}, T_{base}, and T_{ther}. The TGR at the baseline (TGR_{base}) was approximately calculated with the following formula: $TGR_{base}=log_{10}\ (V_{base}/V_{pre})/(T_{base}-T_{pre})$ TGR after ICI treatment (TGR_{ther}) was approximately calculated with the following formula: $TGR_{ther}=log_{10}\ (V_{ther}/V_{base})/(T_{ther}-T_{base})$ HPD was defined as the TGR amplification over 50% in the 2 months after ICI administration and was calculated with the following formula: $(TGR_{ther}-TGR_{base})/TGR_{base}\times100\%\geq50\%$.

Laboratory data

The laboratory data of all patients were collected within 4 weeks before the start of ICI treatment, and no antitumor treatment was performed in the first 4 weeks before testing. The normal ranges of laboratory data were showed in Table S1. The collected laboratory data included measures of blood C reactive protein (mg/mL), D dimer (mg/L), percentage of neutrophils, neutrophil count, lactate dehydrogenase (LDH, U/L), percentage of monocytes, monocyte count, percentage of basophils, basophil count, percentage of eosinophils, eosinophil count, international normalization ratio, large platelet ratio, urea (mmol/L), uric acid (µmol/L), mean red blood cell volume (fl), average hemoglobin content (pg), mean corpuscular hemoglobin concentration (MCHC, pg), mean platelet volume (fl), total cholesterol (µmol/L), total bile acid (µmol/L), total bilirubin (µmol/L), total protein (g/L), chloride ion (mmol/L), activated partial prothrombin time (seconds), lymphocyte percentage, lymphocyte count, triglycerides (mmol/L), carcinoembryonic antigen, albumin ratio, white blood cell count, albumin (g/L), direct bilirubin (µmol/L), alkaline phosphatase (U/L), phosphorus (mmol/L), neuronal specific enolase (ng/mL), glycated albumin (%), glycosylated hemoglobin (%), carbohydrate antigen 125 (U/mL), coefficient of variation of red blood cell distribution width (fl), standard deviation of red blood cell distribution width (fl), hematocrit (%), red blood cell count, fibrinogen (g/L), cytokeratin 19 fragment (ng/mL), myoglobin (ng/mL), creatinine (umol/L), creatine kinase (mmol/L), creatine kinase isoenzyme-MB (mmol/L), troponin I(ng/mL), cholinesterase (KU/L), cystatin c (mg/L), glucose (mmol/L), platelet distribution width (fl), platelet packed volume (fl), platelet count, erythrocyte sedimentation rate (ESR), angiotensin converting enzyme (mm/1h), hemoglobin concentration (g/L), retinol-binding protein (mg/L), superoxide dismutase (mmol/L), calcium (mmol/L), sodium ion (mmol/L), potassium ion (mmol/L), magnesium (mmol/L), aspartate aminotransferase (U/L), high-density lipoprotein (HDL) cholesterol (mmol/L), and squamous cell carcinoma antigen (ng/mL).

Statistical analyses

This study used SPSS 24.0 (IBM Corp., Armonk, NY, USA) and R v. 3.6.3 software (The R Foundation for Statistical Computing, Vienna, Austria) for statistical analyses. Statistical analysis was 2-tailed with 95% confidence interval (CI), and a P value <0.05 was considered statistically different. The difference between the HPD and non-HPD groups was tested with a χ^2 test or Fisher's exact test. Univariate logistic regression analysis was performed in the training set, and statistically significant variables with a P value <0.05 were selected for multivariate logistic regression analysis. The independent risk factors were developed based on the multivariate logic analysis using the rms package in R and were selected to build a nomogram model.

Results

Patient characteristics

For the training set, a total of 1,147 patients were screened, and 844 patients were finally included in the study. The patient screening process is shown in *Figure 1*. For The testing set, a total of 326 patients were screened, and included 211 patients. In the training set, the median time from pre-baseline to baseline in the HPD group was 33 days (20–47 days) and 35 days (17–50 days) in the non-HPD group. After evaluation of the CT scan, 93 patients (11%) were confirmed to have HPD. And testing set included 25 (11.8%) patients with HPD. The baseline data (age, gender, etc.) of training set and testing set are shown in *Table 1*. The age, gender, number of organs with metastases and other clinical situations showed no difference between HPD and non-HPD group.

Logistic regression analyses

The results of univariate logistic regression analyses are shown in Table S2. D-dimer, percentage of neutrophils, neutrophil count, LDH (U/L), MCHC (pg), ESR, neuron specific enolase (ng/mL), hemoglobin concentration (g/L), lymphocyte percentage, and lymphocyte count showed statistically significant differences between the HPD group and the non-HPD group. Subsequently, these variables were included in the next step of multivariate logistics regression analysis using the Enter method (*Table 2*). Finally, in the comparison between HPD patients and non-HPD patients, 3 variables were found to be significant, including LDH [P<0.001; odds ratio (OR) =0.987; 95% CI: 0.980–0.995], MCHC (P=0.038; OR =1.021; 95% CI: 1.003–1.033), and ESR (P=0.012; OR =0.989; 95% CI: 0.977–0.997). These were eventually identified as independent factors that indicated HPD; therefore, the prediction model was established based on these 3 variables.
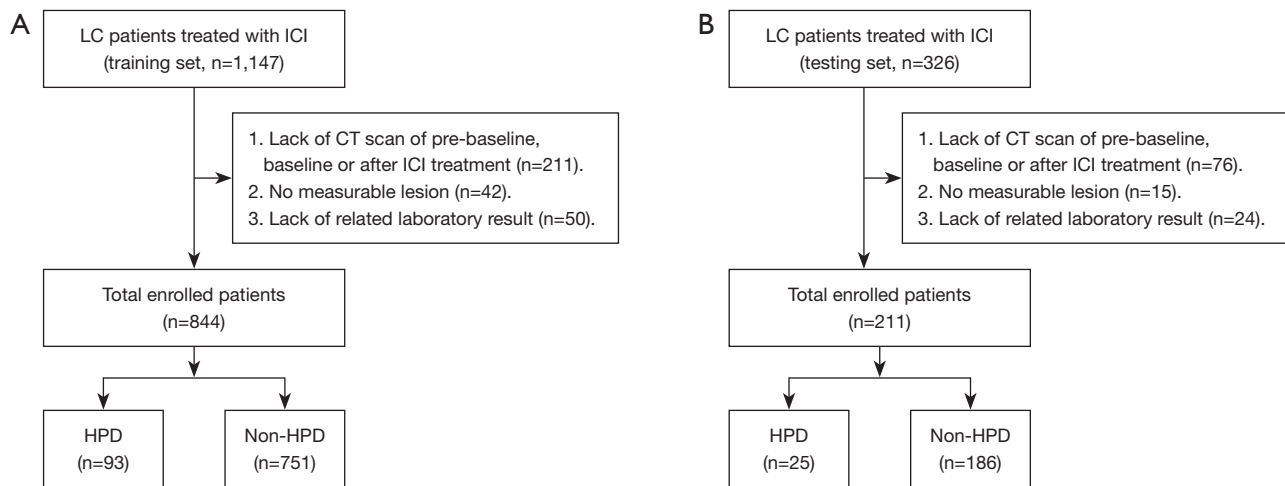
610

Cao et al. Nomogram for predicting hyperprogressive disease

Figure 1 Flowchart of participant selection in the training set (A) and in the testing set (B). LC, lung cancer; ICI, immune checkpoint inhibitor; CT, computed tomography; HPD, hyperprogressive disease.

Table 1 Characteristics of patients in the HPD and non-HPD groups

Variable	Training set (n=844)			Testing set (n=211)		
	HPD (n=93)	Non-HPD (n=751)	P	HPD (n=25)	Non-HPD (n=186)	P
Age ≥65 years, n (%)	34 (36.6)	414 (55.1)	0.147	8 (32.0)	83 (44.6)	0.231
Male, n (%)	73 (78.5)	686 (85.6)	0.068	14 (56.0)	130 (69.9)	0.161
Stage, n (%)			0.905			0.713
I–II	2 (2.2)	19 (2.5)		0 (0.0)	1 (0.5)	
III–IV	91 (97.8)	732 (96.9)		25 (100.0)	185 (99.5)	
ECOG PS, n (%)			0.994			0.411
0–1	89 (95.7)	724 (96.4)		24 (96.0)	183 (98.4)	
2	4 (4.3)	27 (3.6)		1 (4.0)	3 (1.6)	
Smoking, n (%)			0.481			0.908
Current/former	60 (64.5)	508 (67.6)		13 (52.0)	99 (53.2)	
None	33 (35.5)	243 (32.4)		12 (48.0)	87 (46.8)	
Histology, n (%)			0.575			0.997
Adenocarcinoma	47 (50.5)	415 (55.3)		13 (52.0)	100 (53.8)	
Squamous lung cancer	30 (32.3)	239 (31.8)		8 (32.0)	56 (30.1)	
Small cell lung cancer	9 (9.7)	62 (8.3)		2 (8.0)	16 (8.6)	
Others	7 (7.5)	35 (4.7)		2 (8.0)	14 (7.5)	
Therapy lines of ICI, n (%)			0.404			0.455
1	10 (10.8)	64 (8.5)		3 (12.0)	37 (19.9)	
2	56 (60.2)	445 (59.3)		18 (72.0)	131 (70.4)	
≥3	27 (29.0)	242 (32.2)		4 (16.0)	18 (9.7)	

Table 1 (*continued*)

Table 1 (*continued*)

Variable	Training set (n=844)			Testing set (n=211)		
	HPD (n=93)	Non-HPD (n=751)	P	HPD (n=25)	Non-HPD (n=186)	P
PD-L1 status, n (%)			0.668			0.711
<1	5 (5.4)	47 (6.3)		5 (20.0)	37 (19.9)	
1–50%	7 (7.5)	54 (7.2)		3 (12.0)	13 (7.0)	
>50%	2 (2.2)	30 (4.0)		2 (8.0)	9 (4.8)	
Unknown	79 (84.9)	620 (82.5)		15 (60.0)	127 (68.3)	
Molecular status, n (%)			0.492			0.438
EGFR/ALK/ROS-1	4 (4.3)	37 (4.9)		4 (16.0)	20 (10.8)	
Wild type	89 (95.7)	714 (95.1)		21 (84.0)	166 (89.2)	
Organs with metastases, n (%)			0.438			0.881
≤2	82 (88.2)	647 (86.2)		21 (84.0)	154 (82.8)	
≥3	11 (11.8)	104 (13.8)		4 (16.0)	32 (17.2)	
Combination with chemotherapy			0.486			0.725
No	50 (53.8)	490 (65.2)		11 (44.0)	75 (40.3)	
Yes	43 (46.2)	261 (34.8)		14 (56.0)	111 (59.7)	
Antibiotics in 2 weeks			0.511			0.602
Yes	0 (0.0)	29 (3.9)		0 (0.0)	2 (1.1)	
No	93 (100.0)	722 (96.1)		25 (100.0)	184 (98.9)	
Combination with corticosteroid			0.708			0.812
No	59 (63.4)	520 (69.2)		12 (48.0)	94 (50.5)	
Yes	34 (36.6)	231 (30.8)		13 (52.0)	92 (49.5)	
Types of ICIs			0.209			0.536
Nivolumab	34 (36.6)	330 (43.9)		10 (40.0)	69 (37.1)	
Pembrolizumab	42 (45.1)	325 (43.3)		12 (48.0)	104 (55.9)	
Durvalumab	8 (8.6)	32 (4.3)		2 (8.0)	5 (2.7)	
Atezolizumab	9 (9.7)	64 (8.5)		1 (4.0)	8 (4.3)	

HPD, hyperprogressive disease; ECOG PS, Eastern Cooperative Oncology Group, performance status; ICI, immune checkpoint inhibitor; PD-L1, programmed death-1; EGFR, epidermal growth factor receptor; ALK, anaplastic lymphoma kinase; ROS-1, proto-oncogene tyrosine-protein kinase-1.

Nomogram establishment

We used the rms package in R software to construct a nomogram prediction model of the significant predictors selected by the logistics regression, which included LDH, MCHC, and ESR (*Figure 2*). Total scores were calculated using LDH, MCHC, and ESR. The value of each variable was given a score on the point scale axis. The total score was easily calculated by adding up each individual score. By projecting the total score into a lower total subscale, we estimated the risk of HPD. Internal validation was performed to evaluate discrimination and calibration (14). The nomogram showed a powerful prognostic ability of HPD in both training set and testing set. The concordance index of all

612

Cao et al. Nomogram for predicting hyperprogressive disease

Table 2 Multivariate logistics regression analysis (compared to the HPD set)

Laboratory data	Training set (n=844)		Testing set (n=211)	
	P value	OR (95% CI)	P value	OR (95% CI)
D dimer	0.331	0.861 (0.637–1.164)	–	–
Percentage of neutrophils	0.152	0.875 (0.730–1.050)	–	–
Neutrophil count	0.053	3.388 (0.986–11.647)	–	–
Lactate dehydrogenase	<0.001	0.987 (0.980–0.995)	<0.001	0.976 (0.966–0.987)
Mean corpuscular hemoglobin concentration	0.038	1.021 (1.003–1.033)	0.023	1.018 (1.003–1.034)
Erythrocyte sedimentation rate	0.012	0.989 (0.977–0.997)	0.038	0.982 (0.966–0.999)
Neuronal specific enolase	0.543	0.973 (0.889–1.064)	–	–
Hemoglobin concentration	0.122	1.082 (0.979–1.197)	–	–
Lymphocyte percentage	0.867	1.021 (0.803–1.297)	–	–
Lymphocyte count	0.306	4.949 (0.232–105.258)	–	–

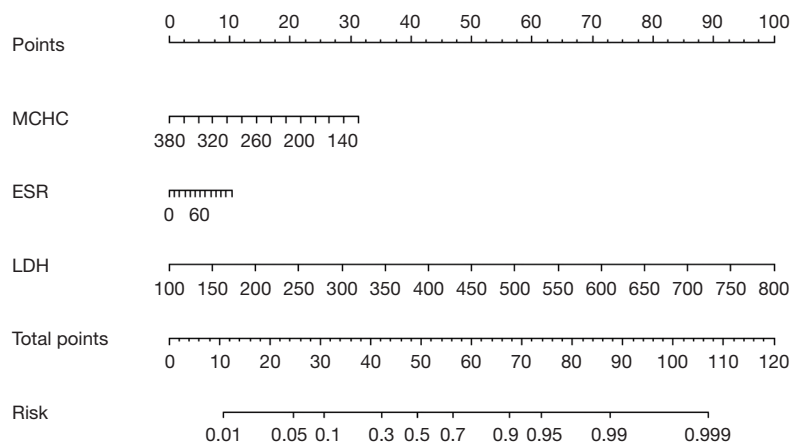HPD, hyperprogressive disease; CI, confidence interval; OR, odds ratio.

Figure 2 Nomogram for the prediction of HPD in LC patients treated with ICIs. MCHC, mean corpuscular hemoglobin concentration; ESR, erythrocyte sedimentation rate; LDH, lactate dehydrogenase; HPD, hyperprogressive disease; LC, lung cancer; ICIs, immune checkpoint inhibitors.

the training data sets was 0.899 (95% CI: 0.859–0.918) and of the testing set was 0.924 (95% CI: 0.866–0.983), suggesting a good discrimination ability. The area under curve (AUC) of the predicted probability is shown in *Figure 3A,3B*. We then assessed the calibration of the model. *Figure 3C* illustrates the calibration curve of the nomogram model. When the predicted probability was between 0.05 and 0.4, the model overestimated the occurrence of HPD; when the predicted probability was lower than 0.05 or higher than 0.4, the model underestimated the HPD rate. Internal validation indicated that the model demonstrated

superior discrimination and acceptable calibration.

Discussion

HPD is one of the response patterns that may appear in the administration of immunotherapy. Accurate prediction of HPD is urgently needed to provide better management of LC patients by screening patients for ICI therapy. In this study, we summarized the common laboratory indicators of 844 patients who had undergone ICI administration, established a prediction model of the HPD population
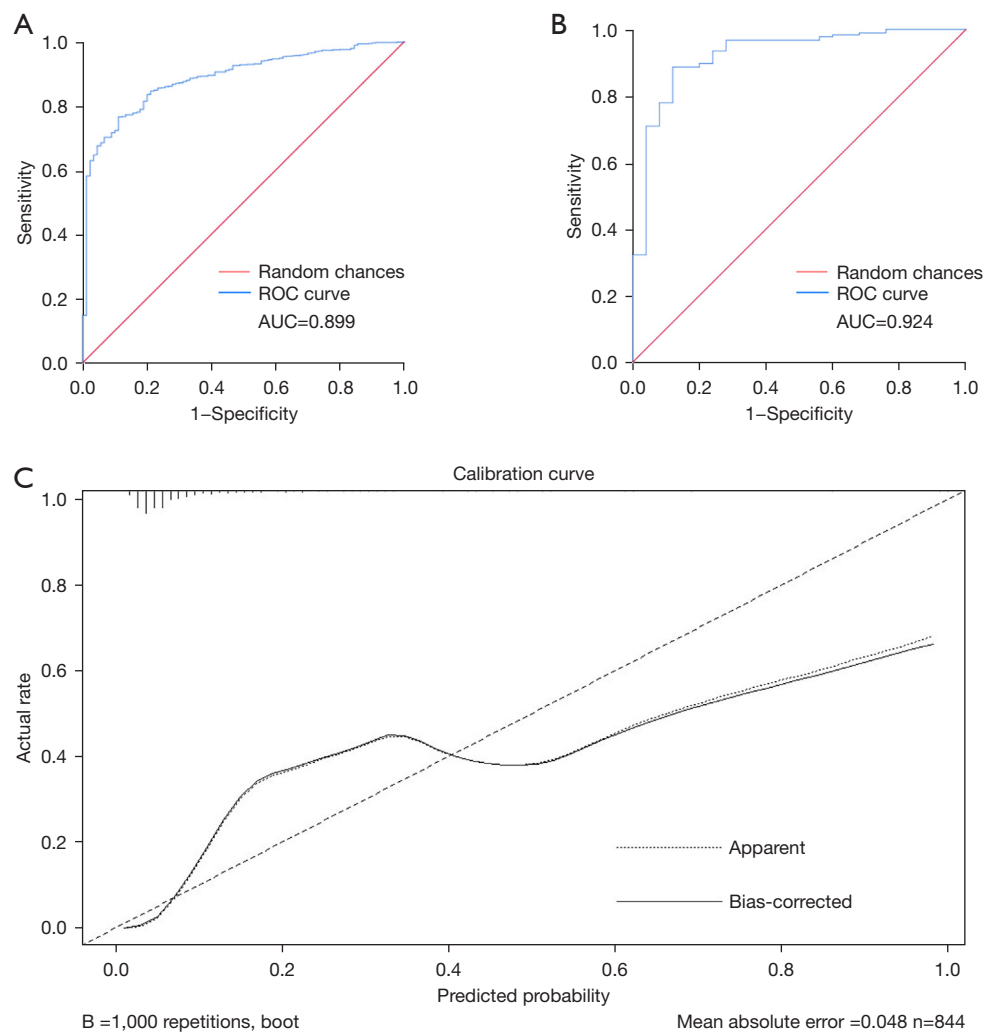
Figure 3 Evaluation of the nomogram model. (A) AUC of the nomogram model in training set; (B) AUC of the nomogram model in testing set; (C) calibration curves of the nomogram model. AUC, area under curve.

based on the significantly different factors between the HPD and non-HPD group, and conducted internal validation. Ultimately, we screened out the 3 most valuable indicators, which were MCHC, ESR, and LDH, and established a nomogram model to quantify the risks of HPD in LC patients who undergo ICI therapy.

HPD is the rapid progression of a disease after the initiation of ICI treatment. In a retrospective study conducted by Ferrara *et al.* (8), 56 of 406 patients who had undergone ICI therapy experienced HPD. The overall survival (OS) of the 56 patients was 3.4 months (95% CI: 2.8–7.5 months), and the median OS of patients without HPD was 6.2 months (95% CI: 5.3–7.9 months). According to previous report, the incidence of HPD is

about 10%, with some reports reaching 20–30% (8,11,15). This discrepancy could possibly be due to the differences in tumor types and different computational approaches of HPD. In the present study, the incidence of HPD was 11%, which was similar to that reported by Ferrara *et al.* (8).

Several studies have explored the possible predictors of HPD. One study found that the expression of FoxP3 high CD45RA-CD4+ T cells (effector Treg) in tumor tissue was related to the occurrence of HPD (16). Lo Russo *et al.* (9) reported that the infiltration of M2 type macrophages may be a biomarker of HPD. They found that the combination of Fc receptor and ICIs could initiate the reprogramming of tumor-associated macrophages, which ultimately leads to HPD. In addition to exploring biomarkers from TME,

studies also found that *MDM2* and *ILC3* gene mutations may be risk factors for HPD (16-19). Li *et al.* (20) found that HPD patients showed more frequent *RAD54L* mutations than non-HPD patients. Other research has also found that advanced age and past field radiotherapy could also be predictors of HPD (7,15), in addition to an elevated absolute serum neutrophil count (ANC) and C-reactive protein (CRP) (21).

Although there have been many differences found in the clinical characteristics between HPD and non-HPD patients, a considerable amount of time may be needed before the relevant biomarkers can be identified. The value of a single index is also limited, and the positive predictive value from a limited index may be low. Few studies have attempted to establish HPD prediction models. An accurate preoperative assessment is critical for appropriately selecting patients suited to ICI; therefore, we used potential biomarkers from generic blood tests. Three meaningful indicators, which were LDH, MCHC, and ESR, were screened out to develop and validate a novel nomogram model for predicting HPD for patients with LC based on the results of univariate and multivariate logistic regression analysis.

Serum LDH status has been demonstrated by multiple studies to be related to the occurrence of HPD. Glycolysis is the main type of energy metabolism through which the rapid proliferation in tumor cells is achieved. In this process, enzymes in the glycolytic pathway, including LDH, are upregulated. In a meta-analysis of advanced non-small cell cancer patients (NSCLC), patients treated with ICIs and who had high pretreatment LDH levels (higher than the upper limit of the normal range) were significantly associated with shorter progression-free survival [hazard ratio (HR) 1.62; 95% CI: 1.26–2.08; P<0.001] and OS (HR 2.38; 95% CI: 1.37–4.12; P=0.002) (22). In a previous study of gastric cancer, HPD patients exhibited a higher level of LDH (23). A systemic review and meta-analysis reported LDH as one of the markers of HPD (24). Kim *et al.*'s (25) study also found that LDH is related to the early occurrence of HPD after ICI application but is not significantly predictive of HPD. In our study, the baseline level of LDH could predict the occurrence of HPD in univariate and multivariate analyses, and it appeared clear that patients with higher LDH levels were more prone to HPD compared to those with lower LDH levels; therefore, we selected LDH as a predictive indicator for the nomogram model.

Qu *et al.* (26) found that a lower level of MCHC

is a prognostic factor of poorer outcomes in patients undergoing lung resection for NSCLC. In addition, patients with a hemoglobin level <12 g/dL may experience poor ICI efficacy (27). Elevated levels of ESR have also been shown to be associated with tumorigenesis and poorer survival, especially in patients with hematologic cancers or colorectal cancers (28,29). For LC, Hannisdal (30) reported that a high ESR was associated with worse survival.

Previous research above has shown that levels of LDH, MCHC, and ESR in blood are associated with the prognosis of LC. Although the correlation between a high level of LDH and HPD has been demonstrated, previous reports have not examined whether MCHC and ESR levels of serum are associated with HPD. However, elevated LDH and ESR, and decreased MCHC, usually reflect a systemic inflammatory state. Therefore, we speculated that the systemic inflammatory state prior to the onset of ICI may trigger HPD after blocking the immune checkpoint signaling. In our study, OR value was near 1 and the P value showed significant effects. The nomogram model based on multivariate logistic analysis had a good discrimination ability and could have a promising predictive ability.

This present study is the first of its kind to develop a HPD patient prediction model based on common clinical laboratory testing. Despite its novelty, some limitations should be noted. First, the retrospective design employed might have introduced selection bias, and the results of the study require verification by a large-scale, prospective study. Moreover, only internal validation was performed, and external validation should be conducted in the future. Furthermore, although we speculated that HPD may be related to personal inflammatory status, we did not test all inflammatory markers in the current study. Meanwhile, sex difference in terms of laboratory test values could be a limitation of this study. And survival differences were unclear between HPD and non-HPD group because the lack of the survival data. Overall, larger, multicenter, prospective trials are needed to validate the results of our study.

In summary, baseline laboratory examination indicators including LDH, MCHC, and ESR have implications for the occurrence of HPD. Building on these results, we established a nomogram model to predict the occurrence of HPD, which showed high sensitivity and specificity. This model may prove effective for screening out those patients who could be at a high risk of developing HPD after ICI therapy. Therefore, this model may have considerable clinical value.

Footnote

Reporting Checklist: The authors have completed the TRIPOD reporting checklist. Available at https://tlcr.amegroups.com/article/view/10.21037/tlcr-22-171/rc

Data Sharing Statement: Available at https://tlcr.amegroups.com/article/view/10.21037/tlcr-22-171/dss

Conflicts of Interest: All authors have completed the ICMJE uniform disclosure form (available at https://tlcr.amegroups.com/article/view/10.21037/tlcr-22-171/coif). SW reports grants or contracts from AztraZeneca and Boehringer Ingelheim, and payment or honoraria from AstraZeneca, Chugai Pharma, Ono Pharmaceutical, Bristol-Myers, Boehringer Ingelheim, Eli Lilly, MSD, Taiho Pharmaceutical, Pfizer, Novartis, and Daiichi Sankyo. NS obtained commercial research grants from Eli Lilly, Chugai Pharmaceutical, Taiho Pharmaceutical, Pfizer Japan, Ono Pharmaceutical, and Nippon Boehringer Ingelheim, and has received speaking honoraria from Eli Lilly, AstraZeneca, MSD Oncology, Chugai Pharmaceutical, Taiho Pharmaceutical, Pfizer Japan, Ono Pharmaceutical, Nippon Boehringer Ingelheim, and Bristol-Myers Squibb Japan. The other authors have no conflicts of interest to declare.

Ethical Statement: The authors are accountable for all aspects of the work in ensuring that questions related to the accuracy or integrity of any part of the work are appropriately investigated and resolved. The study was conducted in accordance with the Declaration of Helsinki (as revised in 2013). The study was approved by institutional ethics board of Shanghai Chest hospital (No. IS2118). Individual consent for this retrospective analysis was waived.

References

1. Siegel RL, Miller KD, Jemal A. Cancer statistics, 2018. CA Cancer J Clin 2018;68:7-30.

2. Goldstraw P, Crowley J, Chansky K, et al. The IASLC Lung Cancer Staging Project: proposals for the revision of the TNM stage groupings in the forthcoming (seventh) edition of the TNM Classification of malignant tumours. J Thorac Oncol 2007;2:706-14.

3. Gettinger S, Horn L, Jackman D, et al. Five-Year Follow-Up of Nivolumab in Previously Treated Advanced Non-Small-Cell Lung Cancer: Results From the CA209-003 Study. J Clin Oncol 2018;36:1675-84.

4. Larkin J, Minor D, D'Angelo S, et al. Overall Survival in Patients With Advanced Melanoma Who Received Nivolumab Versus Investigator's Choice Chemotherapy in CheckMate 037: A Randomized, Controlled, Open-Label Phase III Trial. J Clin Oncol 2018;36:383-90.

5. Ribas A, Wolchok JD. Cancer immunotherapy using checkpoint blockade. Science 2018;359:1350-5.

6. Reck M, Rodríguez-Abreu D, Robinson AG, et al. Pembrolizumab versus Chemotherapy for PD-L1-Positive Non-Small-Cell Lung Cancer. N Engl J Med 2016;375:1823-33.

7. Champiat S, Dercle L, Ammari S, et al. Hyperprogressive Disease Is a New Pattern of Progression in Cancer Patients Treated by Anti-PD-1/PD-L1. Clin Cancer Res 2017;23:1920-8.

8. Ferrara R, Mezquita L, Texier M, et al. Hyperprogressive Disease in Patients With Advanced Non-Small Cell Lung Cancer Treated With PD-1/PD-L1 Inhibitors or With Single-Agent Chemotherapy. JAMA Oncol 2018;4:1543-52.

9. Lo Russo G, Moro M, Sommariva M, et al. Antibody-

Fc/FcR Interaction on Macrophages as a Mechanism for Hyperprogressive Disease in Non-small Cell Lung Cancer Subsequent to PD-1/PD-L1 Blockade. Clin Cancer Res 2019;25:989-99.

10. Matos I, Martin-Liberal J, García-Ruiz A, et al. Capturing Hyperprogressive Disease with Immune-Checkpoint Inhibitors Using RECIST 1.1 Criteria. Clin Cancer Res 2020;26:1846-55.

11. Champiat S, Ferrara R, Massard C, et al. Hyperprogressive disease: recognizing a novel pattern to improve patient management. Nat Rev Clin Oncol 2018;15:748-62.

12. Nishino M, Giobbie-Hurder A, Gargano M, et al. Developing a common language for tumor response to immunotherapy: immune-related response criteria using unidimensional measurements. Clin Cancer Res 2013;19:3936-43.

13. Gomez-Roca C, Koscielny S, Ribrag V, et al. Tumour growth rates and RECIST criteria in early drug development. Eur J Cancer 2011;47:2512-6.

14. Alba AC, Agoritsas T, Walsh M, et al. Discrimination and Calibration of Clinical Prediction Models: Users' Guides to the Medical Literature. JAMA 2017;318:1377-84.

15. Saâda-Bouzid E, Defaucheux C, Karabajakian A, et al. Hyperprogression during anti-PD-1/PD-L1 therapy in patients with recurrent and/or metastatic head and neck squamous cell carcinoma. Ann Oncol 2017;28:1605-11.

16. Kamada T, Togashi Y, Tay C, et al. PD-1+ regulatory T cells amplified by PD-1 blockade promote hyperprogression of cancer. Proc Natl Acad Sci U S A 2019;116:9999-10008.

17. Xiong D, Wang Y, Singavi AK, et al. Immunogenomic Landscape Contributes to Hyperprogressive Disease after Anti-PD-1 Immunotherapy for Cancer. iScience 2018;9:258-77.

18. Nag S, Zhang X, Srivenugopal KS, et al. Targeting MDM2-p53 interaction for cancer therapy: are we there yet? Curr Med Chem 2014;21:553-74.

19. Kato S, Goodman A, Walavalkar V, et al. Hyperprogressors after Immunotherapy: Analysis of Genomic Alterations Associated with Accelerated Growth Rate. Clin Cancer Res 2017;23:4242-50.

20. Li J, Xiang C, Wang Y, et al. The genomic characteristics of different progression patterns in advanced non-small cell lung cancer patients treated with immune checkpoint inhibitors. Ann Transl Med 2021;9:779.

21. Sasaki A, Nakamura Y, Mishima S, et al. Predictive factors for hyperprogressive disease during nivolumab as anti-PD1 treatment in patients with advanced gastric cancer.

Gastric Cancer 2019;22:793-802.

22. Zhang Z, Li Y, Yan X, et al. Pretreatment lactate dehydrogenase may predict outcome of advanced non small-cell lung cancer patients treated with immune checkpoint inhibitors: A meta-analysis. Cancer Med 2019;8:1467-73.

23. Liu J, Wu Q, Wu S, et al. Investigation on potential biomarkers of hyperprogressive disease (HPD) triggered by immune checkpoint inhibitors (ICIs). Clin Transl Oncol 2021;23:1782-93.

24. Kim JY, Lee KH, Kang J, et al. Hyperprogressive Disease during Anti-PD-1 (PDCD1) / PD-L1 (CD274) Therapy: A Systematic Review and Meta-Analysis. Cancers (Basel) 2019;11:1699.

25. Kim SR, Chun SH, Kim JR, et al. The implications of clinical risk factors, CAR index, and compositional changes of immune cells on hyperprogressive disease in non-small cell lung cancer patients receiving immunotherapy. BMC Cancer 2021;21:19.

26. Qu X, Zhang T, Ma H, et al. Lower mean corpuscular hemoglobin concentration is associated with unfavorable prognosis of resected lung cancer. Future Oncol 2014;10:2149-59.

27. Ayers KL, Ma M, Debussche G, et al. A composite biomarker of neutrophil-lymphocyte ratio and hemoglobin level correlates with clinical response to PD-1 and PD-L1 inhibitors in advanced non-small cell lung cancers. BMC Cancer 2021;21:441.

28. Kornum JB, Farkas DK, Sværke C, et al. Cancer Risk and Prognosis after a Hospital Contact for an Elevated Erythrocyte Sedimentation Rate. Cancer Epidemiol Biomarkers Prev 2019;28:225-32.

29. Kantor ED, Udumyan R, Signorello LB, et al. Adolescent body mass index and erythrocyte sedimentation rate in relation to colorectal cancer risk. Gut 2016;65:1289-95.

30. Hannisdal E, Engan T. Blood analyses and survival in symptom- and survey-detected lung cancer patients. J Intern Med 1991;229:337-41.

Table S1 Normal range of all laboratory test

Laboratory data	Normal range
C reactive protein (mg/L)	0.50-10.00
D dimer (mg/L)	0-0.55
Percentage of neutrophils	40.0-75.0
Neutrophil count (10^9/L)	1.8-6.3
Lactate dehydrogenase (U/L)	120-250
Percentage of monocytes	3-10
Monocyte count (10^9/L)	0.1-0.6
Percentage of basophils	0-1.0
Basophil count (10^9/L)	0-0.06
Percentage of eosinophils	0.4-8.0
Eosinophil count (10^9/L)	0-0.5
International normalization ratio	0.8-1.5
Large platelet ratio	13.00-43.00
Urea (mmol/L)	3.1-9.5
Uric acid (µmol/L)	208-428
Mean red blood cell volume (fl)	82.0-100.0
Average hemoglobin content (pg)	27.0-34.0
Mean corpuscular hemoglobin concentration (pg)	316-354
Mean platelet volume (fl)	9.0-13.0
Total cholesterol (µmol/L)	3.0-5.7
Total bile acid (µmol/L)	0-15
Total bilirubin (µmol/L)	5.0-21.0
Total protein (g/L)	65-85
Chloride ion (nmol/L)	99-110
Activated partial prothrombin time (second)	20.1-40.0
Lymphocyte percentage	20.0-50.0
Lymphocyte count (10^9/L)	1.1-3.2
Triglycerides (mmol/L)	0-1.7
Carcinoembryonic antigen (ng/mL)	0-5.00
Albumin ratio	1.20-2.40
White blood cell count (10^9/L)	3.5-9.5
Albumin (g/L)	35-52
Direct bilirubin (µmol/L)	0-3.4
Alkaline phosphatase (U/L)	30-120
Phosphorus (nmol/L)	0.9-1.5
Neuronal specific enolase (ng/mL)	0-25.00
Glycated albumin (%)	11.0-16.0
Glycosylated hemoglobin (%)	4-6
Carbohydrate antigen 125 (U/mL)	0-35.00
Coefficient of variation of red blood cell distribution width (%)	11.0-16.0
Standard deviation of red blood cell distribution width (fl)	37.0-54.0
Hematocrit (%)	35.0-45.0
Red blood cell count (10^{12}/L)	3.8-5.1
Fibrinogen (g/L)	2.0-4.0
Cytokeratin 19 fragment (ng/mL)	0-5.00
Myoglobin (ng/mL)	0-70.0
Creatinine (µmol/L)	57-111
Creatine Kinase (U/L)	50-310
Creatine Kinase Isoenzyme MB (ng/mL)	0.3-0.4
Troponin I (ng/mL)	0-0.03
Cholinesterase (KU/L)	4.6-11.5
Cystatin c (mg/L)	0.5-1.6
Glucose (mmol/L)	4.3-5.9
Platelet distribution width (fl)	9-17
Platelet packed volume (fl)	9.0-13.0
Platelet count	125-350
Erythrocyte sedimentation rate	0-40
Angiotensin converting enzyme (mm/1 h)	18.0-55.0
Hemoglobin concentration (g/L)	115-150
Retinol-binding protein (mg/L)	25-70
Superoxide dismutase (mmol/L)	129-216
Calcium (mmol/L)	2.1-2.5
Sodium ion (mmol/L)	137-147
Potassium ion (mmol/L)	3.5-5.3
Magnesium (mmol/L)	0.75-1.02
Aspartate aminotransferase (U/L)	15-40
HDL cholesterol (mmol/L)	0.8-1.8
Squamous cell carcinoma antigen (ng/mL)	0-1.50

Table S2 Univariate logistic regression analysis (compared to the HPD set)

Laboratory data	P value	OR (95% CI)
C reactive protein (mg/L)	0.516	0.997 (0.988-1.006)
D dimer (mg/L)	0.015	0.924 (0.867-0.985)
Percentage of neutrophils	0.003	0.964 (0.941-0.988)
Neutrophil count	0.032	0.953 (0.913-0.996)
Lactate dehydrogenase (U/L)	0.000	0.986 (0.983-0.990)
Percentage of monocytes	0.323	0.927 (0.799-1.007)
Monocyte count	0.134	0.432 (0.144-1.297)
Percentage of basophils	0.912	1.065 (0.349-3.251)
Basophil count	0.683	0.053 (0.000-73,721.349)
Percentage of eosinophils	0.529	0.964 (0.861-1.080)
Eosinophil count	0.538	0.672 (0.190-2.381)
International normalization ratio	0.770	0.707 (0.069-7.237)
Large platelet ratio	0.939	0.999 (0.968-1.030)
Urea (mmol/L)	0.324	0.903 (0.737-1.106)
Uric acid (µmol/L)	0.404	0.998 (0.995-1.002)
Mean red blood cell volume (fl)	0.923	1.002 (0.955-1.052)
Average hemoglobin content (pg)	0.168	1.086 (0.966-1.222)
Mean corpuscular hemoglobin concentration (pg)	0.004	1.040 (1.013-1.068)
Mean platelet volume (fl)	0.972	0.996 (0.807-1.230)
Total cholesterol (mmol/L)	0.231	0.606 (0.267-1.376)
Total bile acid (µmol/L)	0.510	1.025 (0.953-1.101)
Total bilirubin (µmol/L)	0.403	1.036 (0.953-1.127)
Total protein (g/L)	0.196	0.961 (0.906-1.021)
Chloride ion (nmol/L)	0.620	0.973 (0.872-1.085)
Activated partial prothrombin time (second)	0.663	1.013 (0.957-1.072)
Lymphocyte percentage	0.002	1.058 (1.020-1.097)
Lymphocyte count	0.004	2.188 (1.277-3.749)
Triglycerides (mmol/L)	0.887	1.061 (0.471-2.388)
Carcinoembryonic antigen (ng/mL)	0.646	0.998 (0.989-1.007)
Albumin ratio	0.832	0.868 (0.236-3.197)
White blood cell count	0.082	0.948 (0.893-1.007)
Albumin (g/L)	0.303	0.955 (0.874-1.043)
Direct bilirubin (µmol/L)	0.339	1.150 (0.863-1.532)
Alkaline phosphatase (U/L)	0.306	0.995 (0.987-1.004)
Phosphorus (nmol/L)	0.072	0.104 (0.009-1.221)
Neuronal specific enolase (ng/mL)	0.050	0.993 (0.986-1.000)
Glycated Albumin (%)	0.546	0.949 (0.800-1.125)
Glycosylated hemoglobin (%)	0.551	1.127 (0.638-2.321)
Carbohydrate antigen 125 (U/mL)	0.669	0.999 (0.995-1.003)
Coefficient of variation of red blood cell distribution width (%)	0.204	0.844 (0.650-1.096)
Standard deviation of red blood cell distribution width (fl)	0.557	0.976 (0.902-1.057)
Hematocrit (%)	0.107	1.048 (0.990-1.108)
Red blood cell count	0.697	1.032 (0.881-1.208)
Fibrinogen (g/L)	0.690	0.965 (0.809-1.150)
Cytokeratin 19 fragment (ng/mL)	0.350	0.994 (0.981-1.007)
Myoglobin (ng/mL)	0.878	1.004 (0.955-1.055)
Creatinine (µmol/L)	0.851	0.998 (0.976-1.020)
Creatine Kinase (U/L)	0.626	0.999 (0.997-1.002)
Creatine Kinase Isoenzyme MB (ng/mL)	0.931	0.992 (0.825-1.192)
Troponin I (ng/mL)	0.747	1,017,255.1 (0.000-3.565E+42)
Cholinesterase (KU/L)	0.782	1.028 (0.847-1.246)
Cystatin c (mg/L)	0.280	2.926 (0.416-20.558)
Glucose (mmol/L)	0.342	0.933 (0.809-1.076)
Platelet distribution width (fl)	0.767	0.922 (0.541-1.574)
Platelet packed volume (fl)	0.221	10.286 (0.247-128.838)
Platelet count	0.963	1.000 (0.997-1.003)
Erythrocyte sedimentation rate	0.001	0.989 (0.982-0.996)
Angiotensin converting enzyme (mm/1 h)	0.895	0.989 (0.841-1.163)
Hemoglobin concentration (g/L)	0.026	1.018 (1.002-1.034)
Retinol-binding protein (mg/L)	0.069	0.970 (0.939-1.002)
Superoxide dismutase (mmol/L)	0.833	0.995 (0.950-1.042)
Calcium (mmol/L)	0.413	2.896 (0.227-36.908)
Sodium ion (mmol/L)	0.620	1.029 (0.918-1.154)
Potassium ion (mmol/L)	0.903	1.057 (0.435-2.567)
Magnesium (mmol/L)	0.307	0.052 (0.000-15.075)
Aspartate aminotransferase (U/L)	0.256	1.026 (0.982-1.073)
HDL cholesterol (mmol/L)	0.163	12.589 (0.359-440.929)
Squamous cell carcinoma antigen (ng/mL)	0.873	0.993 (0.911-1.083)

CI, confidence interval; OR, odds ratio.